AIP Conference Proceedings

Controlled defect on multilayer graphene surface by oxygen plasma

Cite as: AIP Conference Proceedings **1788**, 030117 (2017); https://doi.org/10.1063/1.4968370
Published Online: 03 January 2017

Marriatyi Morsin, Suhaila Isaak, Marlia Morsin, et al.

View Online

Export Citation

ARTICLES YOU MAY BE INTERESTED IN

Precise control of defects in graphene using oxygen plasma
Journal of Vacuum Science & Technology A **33**, 060602 (2015); https://doi.org/10.1116/1.4926378

Fabrication of InN on epitaxial graphene using RF-MBE
Journal of Applied Physics **126**, 045301 (2019); https://doi.org/10.1063/1.5092826

Self healing of defected graphene
Applied Physics Letters **102**, 103107 (2013); https://doi.org/10.1063/1.4795292

New
Trailblazers.
Meet the Lock-in Amplifiers that measure microwaves.
1.8 GHz
8.5 GHz
Zurich Instruments
Find out more

AIP Publishing

© 2016 Author(s).

Controlled Defect on Multilayer Graphene Surface by Oxygen Plasma

Marriatyi Morsin[1, b)], Suhaila Isaak[1, c)], Marlia Morsin[2, d)] and Yusmeeraz Yusof[1, a)]

[1]*Department of Electronics and Computer Engineering, Faculty of Electrical Engineering, Universiti Teknologi Malaysia, 81310 UTM, Johor Bahru, Johor, Malaysia*
[2]*Microelectronics & Nanotechnology - Shamsuddin Research Centre (MiNT-SRC), Institute of Integrated Engineering (I2E),Universiti Tun Hussein Onn Malaysia, 86400 Parit Raja, Batu Pahat Johor, Malaysia*

[a)]Corresponding author: yusmeeraz@utm.my
[b)]marriatyi2@live.utm.my
[c)]suhaila@utm.my
[d)]marlia@uthm.edu.my

Abstract. The study pertaining defect fabrication of graphene has gained interest nowadays. To date, the fabrication of the defect using reactive ion etching on the oxygen flow rate has not been adequately studied. In this work, fabrication defect on multilayer graphene using reactive ion etching at 30 sccm and 50 sccm oxygen flow rates as a controlled parameter. The other parameters such as pressure, exposure time and power are set as well. The resistance of the exposed multilayer graphene devices at 30 sccm and 50 sccm are respectively 38 and 49 times higher than the non-exposed device. The increased oxygen flow rate in the reactive ion etching deteriorates the crystalline quality of the multilayer graphene thus declines its function as a device. It is suggested that only low oxygen flow rate is to be used to fabricate small amount of defect for the controlled defect purposes.

INTRODUCTION

Research on graphene pertaining to its physical and electronic properties has been tremendous, since the discovery of graphene in 2004 [1]. Several studies had shown superiorities of graphene, such as higher electron mobility [1], [2], wide electrical window [2], the bareness of the graphene and exposure directly to liquid [2], highly thermal conductance [3], tunable bandgap [2] and zero bandgap [4]. The presence of the conical shape at the Dirac point makes graphene very competitive in electronics application. A pristine graphene device has mobility as high as 10^5 $cm^2/V\text{-}s$ [1] compared to conventional silicone device mobility ≤ 1400 $cm^2\ V^{-1}s^{-1}$. Due to the fact that graphene is a 2-dimensional material that has high ballistics electronic transport [1], many efforts have been done to show the great potential of graphene as sensing and detection device. Despite the outstanding properties, one cannot exclude the potential defect present on graphene surface [5].

Recently, defected graphene field-effect transistor (GFET) for sensor application has been extensively investigated. One of the sensor applications was to sense nitrogen dioxide gas (NO_2) by Hajati *et al* [6], where the study proved that the defect can improve the gas sensing activity. It has been shown experimentally that defects on the graphene gas sensor can achieve 32% of the sensitivity of NO_2 at 600s compared to pristine at only 11% of sensitivity at 900s of detection. It shows the sensitivity almost four times higher compared to pristine on NO_2 detection.

Several techniques to introduce defect on graphene have being done including atom bombardment [7], ion irradiation [6], focused e-beam [8], plasma treatment [9], [10] and pulse-voltage injection[11]. Among all, plasma treatment is a common tool to introduce defect. However, many aspects of the disorder generated by this technique

International Conference on Engineering, Science and Nanotechnology 2016 (ICESNANO 2016)
AIP Conf. Proc. 1788, 030117-1–030117-6; doi: 10.1063/1.4968370
Published by AIP Publishing. 978-0-7354-1452-5/$30.00

remain to be better understood especially in multilayer graphene. Study shows that oxygen plasma is very aggressive and usually result in drastic changes of the structural and electronic properties of graphene even at a short time of exposure [9]. Thus in this study, different oxygen plasma flow rate is used to gradually induced disorder in chemical vapor deposition (CVD) multilayer graphene and atomic force microscopy (AFM) is applied to cater the evolution of the disorder. The functionality of the multilayer graphene before and after oxygen plasma treatment as a device has also been observed in term of current-voltage characteristics.

EXPERIMENTAL METHOD

The experiments were divided into two main sections. The first section was the fabrication of the metal contact and the second section was the reactive etching process on the chemical vapor deposition (CVD) multilayer graphene. In the first section, the vacuum deposition device system (Ulvac Kiko, model VPC-061) was used to form aluminum (Al) metal contact on graphene. As shown in Fig. 1 (a), the Al metal contact was formed at vacuum pressure level 4.99×10^{-3} Pa, current 35 A and voltage 1.7 V at exposure time 2 s. In this case, the dimension of the CVD multilayer graphene is 5 mm per sample. The size of the Al contact is 2 mm × 1 mm with the thickness of 100 µm. The length and width of the multilayer graphene samples are 2mm and 3mm respectively.

For the second part of the experiments, the reactive ion etching (RIE) system CCP type discharge (SNTEK, model BEP5002) was used to fabricate the defect on each samples. In this case, oxygen plasma was released and exposed directly to the samples surface as shown in Fig. 1(b). Kapton tape is patched along with the paper, to cover the Al metal contact from direct oxidation. While the purpose of the paper is to ensure the Al metal contacts do not detach from the sample when the kapton tape is peeled off. The parameters set for the plasma treatment were 30 sccm and 50 sccm for the oxygen flow rates with the power setting of 50 Watt, the pressure of 200mTorr and time exposure of 5s.

After the plasma treatment, the samples were characterized using atomic force microscopy (AFM) (XE-100, Korea) and 2-point probe from Keithley was used to measure the electrical property of the graphene device.

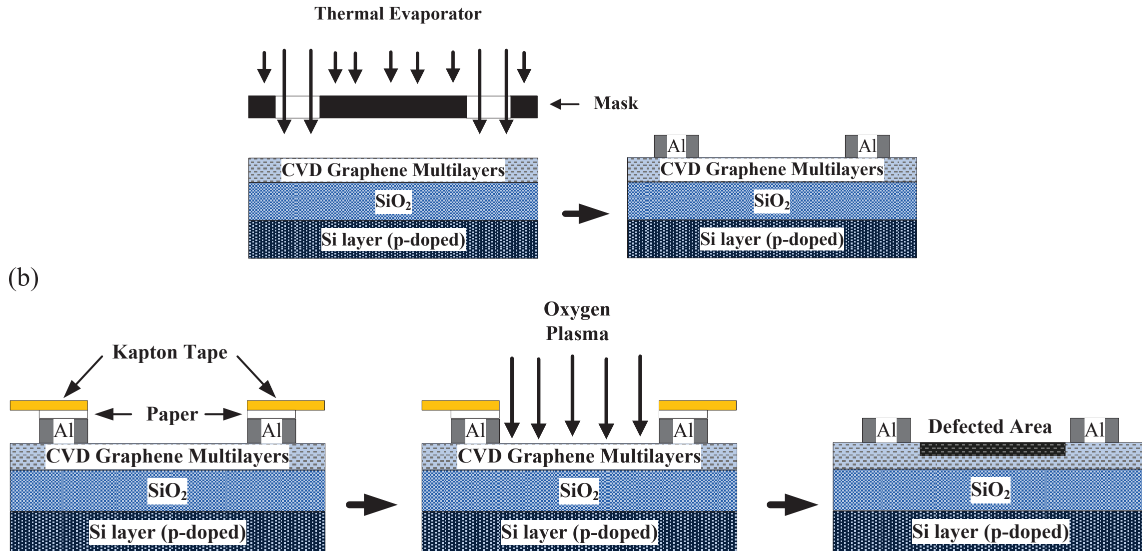

FIGURE 1. Fabrication process of (a) the Al metal contact and (b) the formation of the defects on the CVD multilayer graphene

RESULTS AND DISCUSSION

This section will discuss the results from the experiments gathered from the AFM and the 2-point probe measurement. The results are consist of the discussions about the pristine, the 30 sccm and 50 sccm oxygen flow rates exposed to the multilayer graphene samples.

Atomic Force Microscopy Characterization

AFM is a technique used to characterize the nanoscale surface base developed by Binning and Roher [12]. This technique is used to better understand the morphology of a surface quantitatively [12]. In this study, the results gained from AFM are the 3-D morphology images, the histogram and the line-profile analysis.

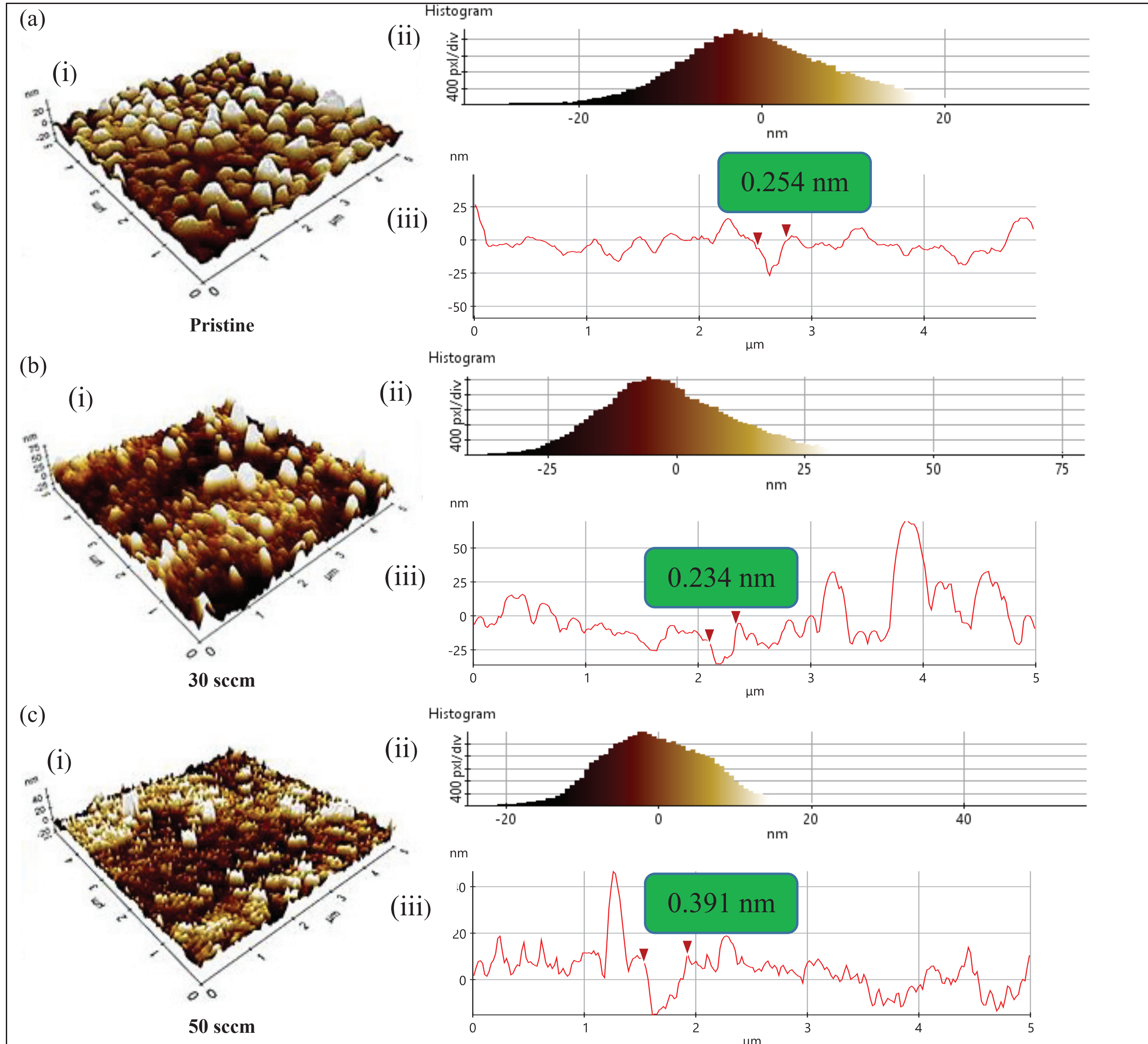

FIGURE 2. The morphology, histogram and line profile of AFM images for (a) pristine, (b) 30 sccm and (c) 50 sccm. (a) (i) - (c)(i) shows the morphology of the AFM images of the respectively samples. (a)(ii) – (c)(ii) shows the histogram of the peaks and the valleys. (a)(iii) – (c)(iii) shows the line profile analysis.

First, the morphology of the graphene samples in pristine, and after the oxygen plasma treatment are observed. As shown in Fig. 2 (a)(i), qualitatively, the pristine shows the most homogenous peaks compared to the graphene samples exposed to the oxygen plasma treatment in Fig. 2 (b)(i) and (c)(i). This topographic contrast can be observed from the peaks (white colors) and the dark brown colors for the valleys distribution. The morphology also shows that the grains size is almost uniform in pristine in opposition to the exposed samples which the grains size is smaller or in spike formed.

To explain more about the distribution of the peak and the valleys in the samples, the histogram Fig. 2 (a)(ii) – (c)(ii) exhibits normal distribution. From the histogram images of Fig. 2 (a)(ii) and (b)(ii), it is shown that the skewedness of the pristine sample and the 30 sccm sample are different. For pristine, the distribution is more to the right, which means the number of the peaks are at large. In contrast to the 30 sccm sample, the skewedness is slightly to the left. The peaks for each samples are between 20 nm to 25 nm high respectively while the valleys are between -20 nm to -25 nm depth respectively. While for the 50 sccm we can see that the peaks and valleys are approximately at 20 nm and -20 nm respectively. This peak reduction may due to the etching process that has etched some layers on the multilayer graphene samples or maybe due to the shrinkage or bending of the sample [13].

The analysis of AFM continues with the line profile analysis. The roughness of the samples due to the oxygen plasma treatment is revealed in the line profile of each sample in Fig. 2 (a)(iii) – (c)(iii). The height of the peaks and the depth of the valleys are clearly shown as well as the measurable distance (size) of the peaks and valleys. In the sample, the size of the peaks and valleys shows rapid changes as the grains size changed.

Figure 3 shows the relationships of the surface roughness towards the oxygen flow rate. The surface roughness values were taken from the RMS roughness and the average roughness of the samples. The average roughness and the RMS roughness is significantly affected by the numbers of peaks and valleys in the image [12]**.** The values of RMS roughness and average roughness show the same trend as it decreased obviously.

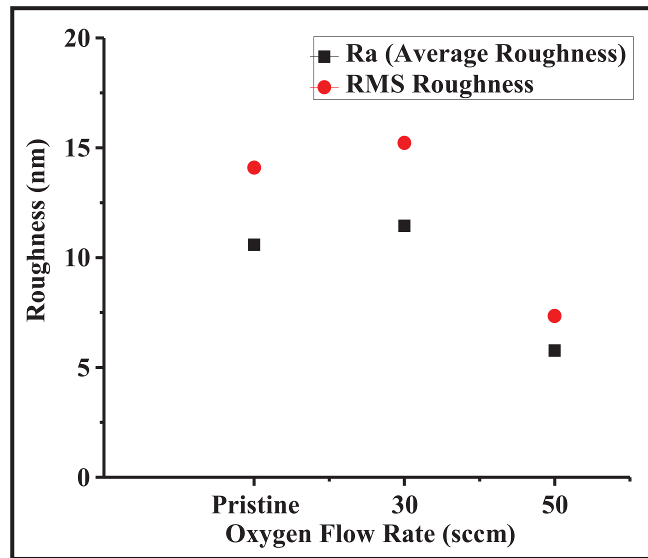

FIGURE 3. The average roughness and the RMS roughness of the pristine and exposed multilayer graphene

Current – Voltage Characteristics

The current – voltage characteristics is done to gain more information about the effect of surface roughness due to oxygen plasma treatment. Fig. 4 shows the current-voltage characteristic of the multilayer graphene with Al metal contact. It is obviously shows that the multilayer graphene either in pristine or exposed to 30 sccm and 50 sccm oxygen plasma which exhibits ohmic behaviour. Among these three samples, the pristine shows the highest ohmic behavior compared to the graphene multilayer device exposed samples. From this figure, the resistance and conductance are calculated and then are tabulated in Table 1. From Table 1, the resistance of multilayer graphene device strongly affected by the amount of flow rates of oxygen plasma, thus decreasing the conductance of the multilayer device. This finding is supported by the study from K. Kim *et al* [14], which reported that the conductance of graphene device can be attributed to the structural defects introduced by the oxygen plasma.

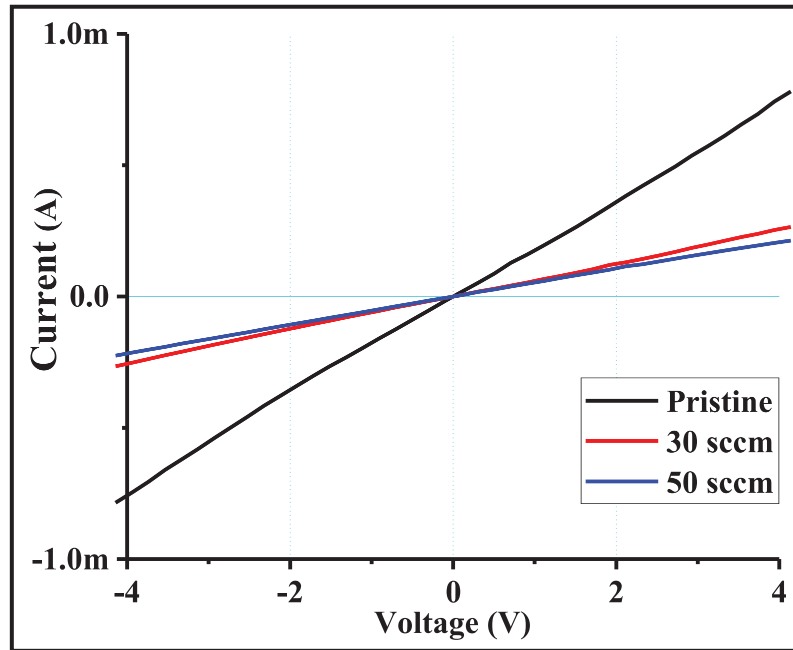

FIGURE 4. Current-voltage characteristics of multilayer graphene for pristine, 30 sccm and 50 sccm respectively.

TABLE 1. The calculated resistance and conductance for pristine, 30sccm and 50 sccm oxygen flow rate device.

Flow Rate (sccm)	Resistance (kΩ)	Conductance (μS)
Pristine	5.25	190.47
30	15.01	66.62
50	19.24	51.97

CONCLUSION

The study was to demonstrate the effect of the reactive ion etching using different controlled oxygen plasma flow rates on the CVD multilayer graphene. The fabricated defects on the graphene samples were characterized using the AFM and the electrical properties were measured afterward. From the study, it shows that the resistance of the exposed graphene samples declined with the crystalline quality of the graphene samples thus deteriorates the its function as a device. It is suggested that only low flow rate is to be used to fabricate small amount of defect on multilayer graphene for the controlled defect purpose. Further study needs to be done to explore extended defect structure that may provide to new physical effects and device concept.

ACKNOWLEDGMENTS

Authors would like to acknowledge the financial support from university research grant of the Ministry of Higher Education (MOHE) of Malaysia under Project Fundamental Research Grant Scheme vote number R.J130000.7823.4F271 and R.J130000.7823.4F269, the Microelectronic and Nanotechnology- Shamsudin Research Center, UTHM, Dr. Feri Adriyanto and Ms. Faezahana Mokhter for the technical support. Also, thanks to the Research Management Center (RMC) of Universiti Teknologi Malaysia (UTM) for providing an excellent research environment to complete this work.

REFERENCES

1. K.S. Novoselov, A.K. Geim, S.V. Morozov, D. Jiang, Y. Zhang, S.V. Dubonos, I.V. Grigorieva and A A. Firsov, Science **306** (5696), 666–669 (2004).
2. K. Matsumoto, K. Maehashi, Y. Ohno and K. Inoue, J. Phys. D. Appl. Phys. **47(9)**, 094005 (2014).
3. A.A. Balandin, S. Ghosh, W. Bao, I. Calizo, D. Teweldebrhan, F. Miao and C.N. Lau, Nano Lett. **8**, 902–907 (2008).
4. M. Pumera, Mater. Today **14(7–8)**, 308–315 (2011).
5. L.D. Carr and M.T. Lusk, Nat. Publ. Gr. **5(5)**, 316–317 (2010).
6. Y. Hajati, T. Blom, S.H.M. Jafri, S. Haldar, and S. Bhandary, "Improved gas sensing activity in structurally defected bilayer graphene," vol. 505501.
7. G. Xie, R. Yang, P. Chen, J. Zhang, X. Tian, S. Wu, J. Zhao, M. Cheng, W. Yang, D. Wang, C. He, X. Bai, D. Shi and G. Zhang, Small **10(11)**, 2280–2284 (2014).
8. T. Xu, X. Xie and L. Sun, "Fabrication of nanopores using electron beam," *8th Annu. IEEE Int. Conf. Nano/Micro Eng. Mol. Syst.*, vol. 1, pp. 637–640, April 2013.
9. A. Felten, A. Eckmann, J.-J. Pireaux, R. Krupke, and C. Casiraghi, Nanotechnology **24(35)**, 355705 (2013).
10. I. Childres, L.A. Jauregui, J. Tian and Y.P. Chen, New J. Phys. **13** (2011).
11. I. Yanagi, R. Akahori, T. Hatano and K. Takeda, Sci. Rep. **4**, 5000 (2014).
12. M. Raposo, Q. Ferreira, and P.A. Ribeiro, Mod. Res. Educ. Top. Microsc. **1**, 758–769 (2007).
13. N. Peltekis, S. Kumar, N. McEvoy, K. Lee, A. Weidlich and G.S. Duesberg, Carbon N.Y. **50(2)**, 395–403 (2012).
14. K. Kim, H.J. Park, B.-C. Woo, K.J. Kim, G.T. Kim and W.S. Yun, Nano Lett. **8(10)**, 3092–3096 (2008).